Supporting Information

Functional Group Engineering in Metalloporphyrin-Based Covalent Organic Framework for Enhanced Sensing Performance

Jia-Li Jian,[abc] Tian-Hao Wang,[abc] Yi-Ming Xu,[b] Jiang-Feng Lu,[b] Guan-E Wang,[bd] Gang Xu,*[bd] and Yong-Jun Chen*[b]

[a]College of Chemistry, Fuzhou University, Fuzhou Fujian 350116, P. R. China.
[b]State Key Laboratory of Structural Chemistry, Fujian Provincial Key Laboratory of Materials and Techniques toward Hydrogen Energy, Fujian Institute of Research on the Structure of Matter, Chinese Academy of Sciences (CAS), Fuzhou, Fujian 350002, P. R. China.
[c]Fujian College, University of Chinese Academy of Science, Fuzhou, Fuzhou, Fujian 350002, P. R. China.
[d]University of Chinese Academy of Sciences (UCAS) Beijing 100049, P. R. China.

*Correspondence and requests for materials should be addressed to G. X. (email: gxu@fjirsm.ac.cn) and Y.-J. C. (email: chenyongjun@fjirsm.ac.cn).

Materials and Methods

Materials

All solvents and reagents obtained from commercial sources were used without further purification. Copper(II) acetate monohydrate ($Cu(CH_3COO)_2 \cdot H_2O$, 99%), 5,10,15,20-tetrakis (4-aminophenyl) porphyrin (TAPP, ≥95%) and mesitylene (97%) were purchased from Aladdin. Terephthalaldehyde (98%), 2,5-dichloroterephthalaldehyde (98%), and 2,5-dimethoxyterephthalaldehyde (98%) were purchased from Adamas-beta. Acetic acid (HAc, AR), N,N-dimethylformamide (DMF, AR), methanol (AR), chloroform (AR), and tetrahydrofuran (THF, AR) were purchased from Sinopharm Chemical Reagent Co., Ltd.

Characterization and instruments

Powder X-Ray diffraction (PXRD) patterns of samples were carried out on a Rigaku SmartLab (Japan) equipped with Cu Kα radiation (λ = 1.54060 Å). The scanning electron microscopy (SEM, ZEISS Sigma 500) and transmission electron microscope (TEM, JEM-F200) were applied to investigate the morphology of the samples. The date of X-ray photoelectron spectroscopy (XPS) was collected from a Thermo Scientific ESCALAB 250 Xi XPS system. A xenon arc lamp (PLS-SXE300D) with a light filter (420-760 nm) was utilized as an irradiation source.

Methods

Synthesis of Cu-TAPP

The synthesis of Cu-TAPP follows previously reported method[1]. 5,10,15,20-tetrakis (4-aminophenyl) porphyrin (200 mg, 0.3 mmol) and $Cu(CH_3COO)_2 \cdot H_2O$ (239.58 mg, 1.2 mmol) were added in a 250 mL three-neck round-bottomed flask. After purification with nitrogen gas for three times, a mixture of methanol (20 mL), chloroform (90 mL) and DMF (30 mL) was added. The flask was heated at 80 ℃ under nitrogen atmosphere stirring and for 24 h. After cooling to room temperature, the solution was transferred into a separatory funnel and washed with water (3 × 100 mL). The dark purple solid was collected through rotary evaporation the above solution.

Synthesis of Cu-COF-366-H

The synthesis method was modified from a previous report[1].Mesitylene (8 mL)

and acetic acid (1.2 mL 6 M) were added to the mixture of terephthalaldehyde (5.6 mg, 0.04 mmol) and Cu-TAPP (14.7 mg, 0.02 mmol) in a 20 mL reactor and sonicated for 15 min. The reactor was heated at 120 ºC under static conditions. After 72 h, the product was obtained. The sample was washed with THF for 3 times. After drying at 65 ºC for 24 h, **Cu-COF-366-H** was obtained.

Synthesis of Cu-COF-366-Cl and Cu-COF-366-OCH_3

For the synthesis of Cu-COF-366-Cl and Cu-COF-366-OCH_3, the procedures were similar to that of Cu-COF-366-H, with the exception that terephthalaldehyde (5.6 mg, 0.04 mmol) was replaced by 2,5-dichloroterephthalaldehyde (10.2 mg, 0.05 mmol) and 2,5-dimethoxyterephthalaldehyde (9.7 mg, 0.05 mmol).

Gas sensor characterization

The gas sensor characterization was conducted by a home-made system reported in our previous work[2]. It took ~0.65 min to fulfill the quartz chamber when the gas flow was 600 mL min^{-1}. The target gas was introduced (3 min) into the quartz tube by mixing the certified gas ‘‘mixtures’’ (Beijing Hua Yuan Gas Chemical Industry Co., Ltd., China) and dry air in a proper ratio controlled by the mass flow controllers (CS-200C, Beijing Sevenstar Qualiflow Electronic Equipment Manufacturing Co., Ltd., China) under visible-light irradiation (λ = 420-760 nm) and room temperature. The constant flow was 600 mL min^{-1}, the bias on the sensor was 5 V and the current was recorded using Keithley 4200 Sourcemeter.

The sensor response with a positive response is defined as the ratio of sensor resistance in the air (R_{air}) and analytic gas ($R_{analyte}$):

$$\text{Response} = R_{air}/R_{analyte} - 1$$

The sensor response with a negative response is defined as the ratio of sensor resistance in the analytic ($R_{analyte}$) and air gas (R_{air}):

$$\text{Response} = R_{analyte}/R_{air} - 1$$

Since the sensing behavior in this work exhibits a negative response, the formula for negative response was adopted:

$$\text{Response} = R_{analyte}/R_{air} - 1$$

The response time ($t_{res.}$) of the sensor with a positive response is the time required

for the increasing current to 90% of the saturation value and the recovery time ($t_{rec.}$) is the time required to decrease the saturated current to its 10%.

The coefficient of variation (CV) is used to represent the change of different cycles on responses, which is defined as:

$$CV = R_{SD}/R_{average} \times 100\%$$

R_{SD} and $R_{average}$ are the standard deviation (SD) and an average value of responses with different cycles at same concentration, respectively.

Theoretical calculation details

In this study, DFT calculations were performed using the DMol3 module within the Materials Studio software package to systematically investigate the effect of different functional group substitutions on the internal charge transfer behavior of the Cu-COF-366-X (X = Cl, H, OCH_3) series materials. The calculations were carried out using the Perdew-Burke-Ernzerhof (PBE) functional within the generalized gradient approximation (GGA). The convergence criteria were set as follows: energy convergence threshold of 1.0×10^{-5} Ha, maximum force convergence threshold of 0.002 Ha/Å, and maximum displacement convergence threshold of 0.005 Å. To systematically investigate the regulatory role of different functional groups on charge transfer, three representative model systems were constructed: Cu-COF-366-Cl bearing an electron-withdrawing substituent (-Cl) on the phenyl ring, unsubstituted Cu-COF-366-H, and Cu-COF-366-OCH_3 bearing an electron-donating substituent (-OCH_3) on the phenyl ring. Hirshfeld charge analysis was employed to quantitatively evaluate the atomic charge distribution and charge transfer behavior of the above models.

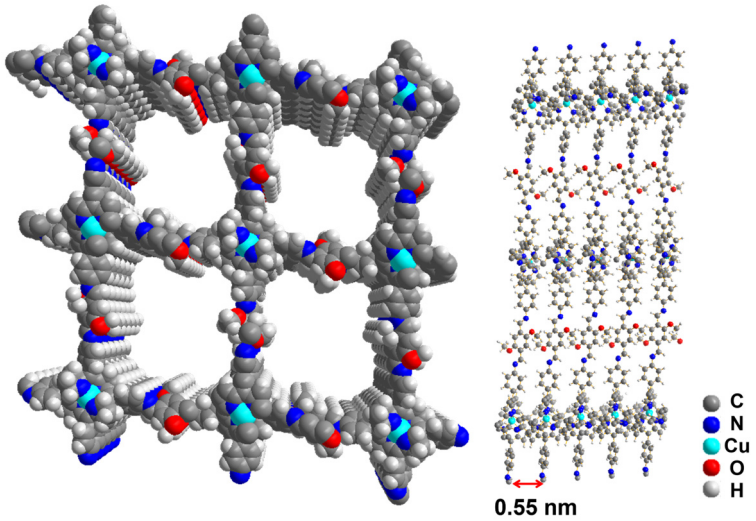

Figure S1. Structure of Cu-COF-366.

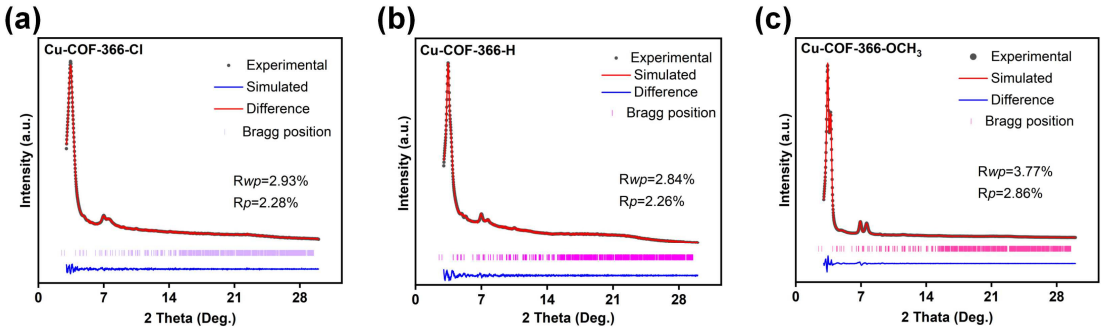

Figure S2. Experimental and simulated PXRD patterns: (a) Cu-COF-366-Cl; (b) Cu-COF-366-H; (c) Cu-COF-366-OCH_3.

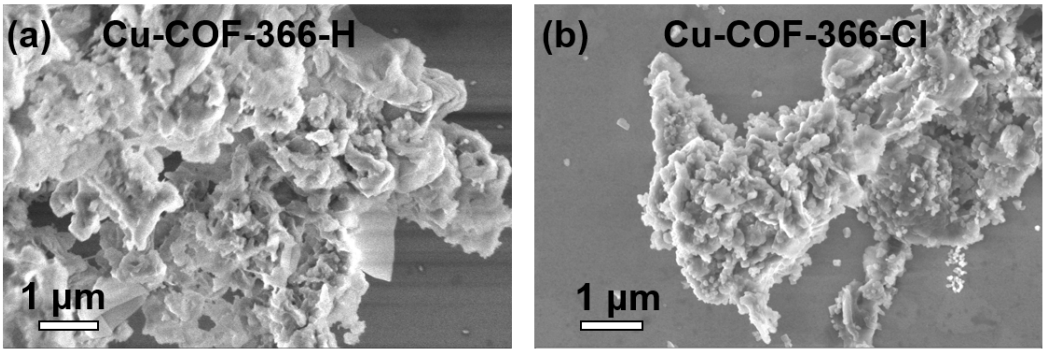

Figure S3. SEM images of Cu-COF-366-H and Cu-COF-366-Cl.

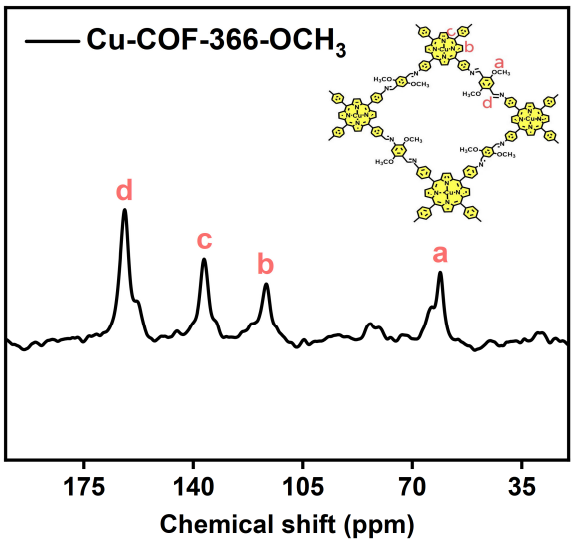

Figure S4. solid-state ^{13}C NMR spectroscopy of Cu-COF-366-OCH_3.

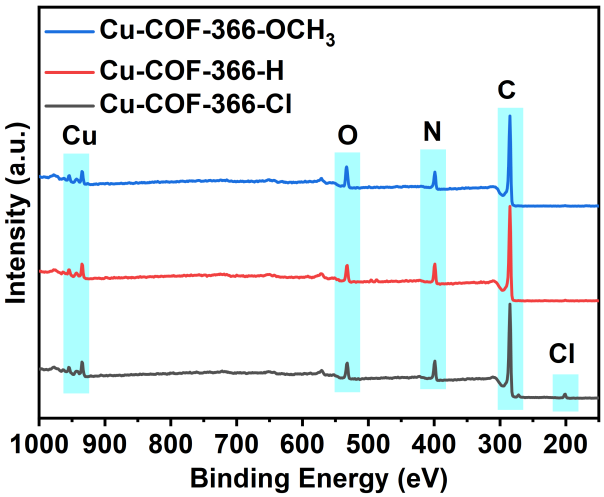

Figure S5. X-ray photoelectron spectroscopy (XPS) of Cu-COF-366-X (X = H, Cl, and OCH_3).

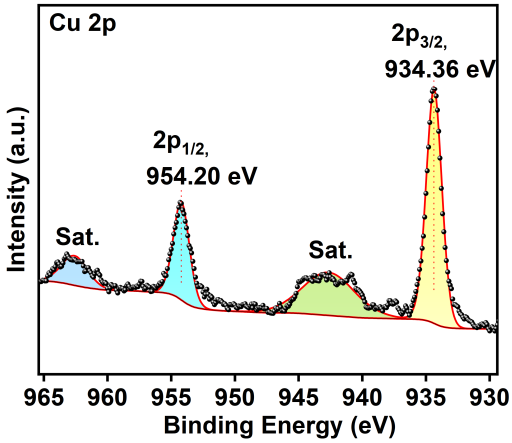

Figure S6. High-resolution Cu 2p X-ray photoelectron spectroscopy of Cu-COF-366-OCH_3.

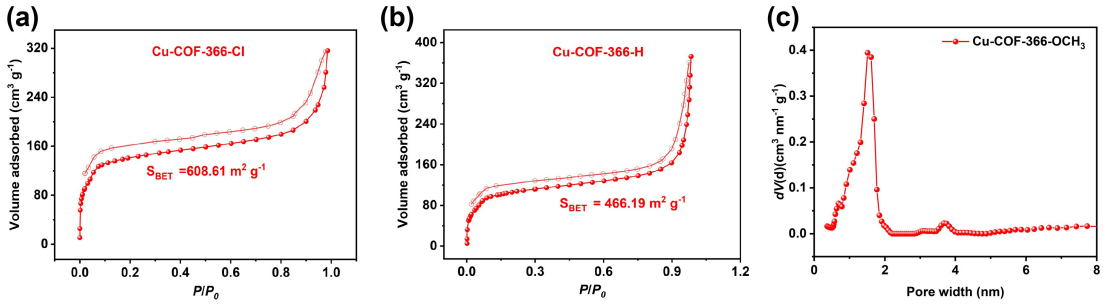

Figure S7. N_2 adsorption isotherms of (a) Cu-COF-366-Cl and (b) Cu-COF-366-H; (c) Pore size distribution curve of Cu-COF-366-OCH_3.

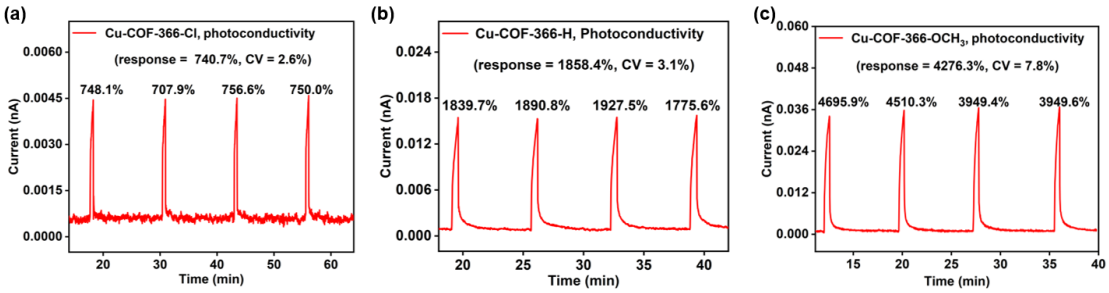

Figure S8. Photoconductivity test of Cu-COF-366-X (X = H, Cl, and OCH_3).

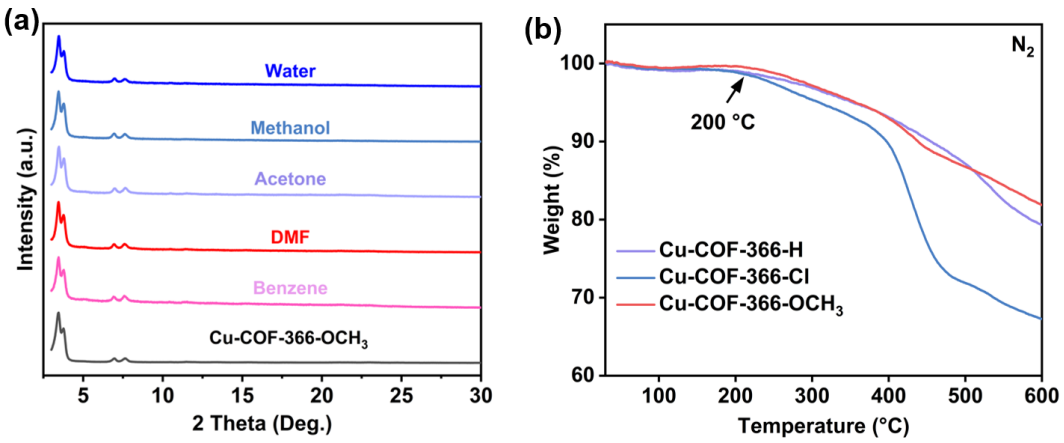

Figure S9. Stability test: (a) chemical stability of Cu-COF-366-OCH_3. (b) Thermal stability of Cu-COF-366-X (X = H, Cl, and OCH_3).

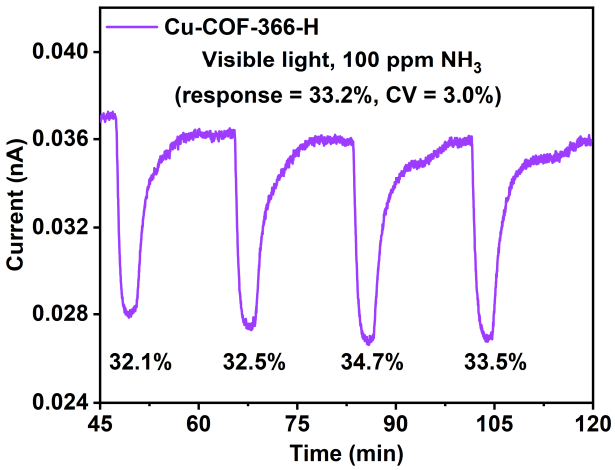

Figure S10. Response-recovery curve of Cu-COF-366-H toward 100 ppm NH_3.

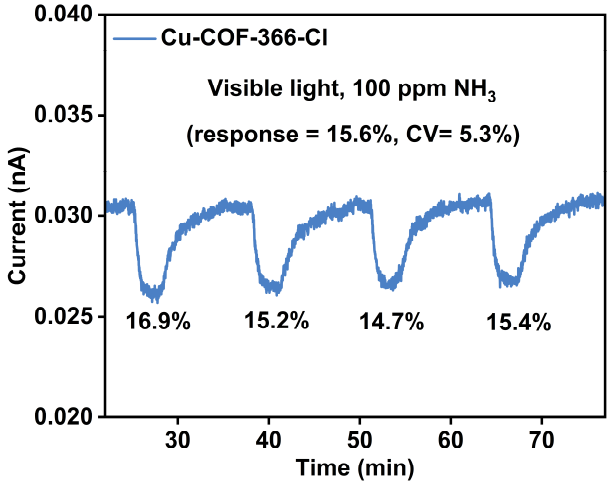

Figure S11. Response-recovery curve of Cu-COF-366-Cl toward 100 ppm NH_3.

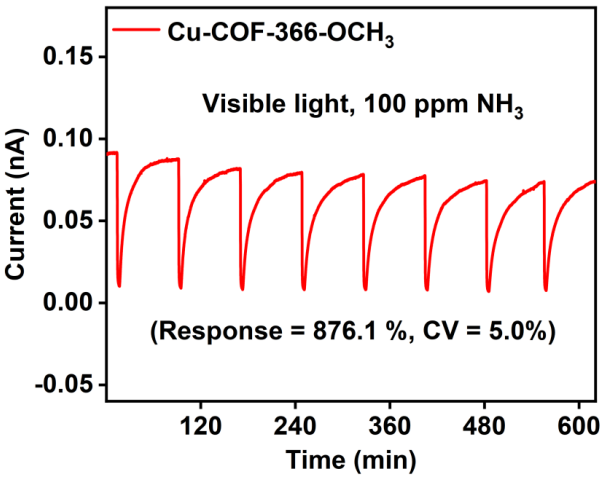

Figure S12. Recycle sensing of Cu-COF-366-OCH_3 towards 100 ppm NH_3.

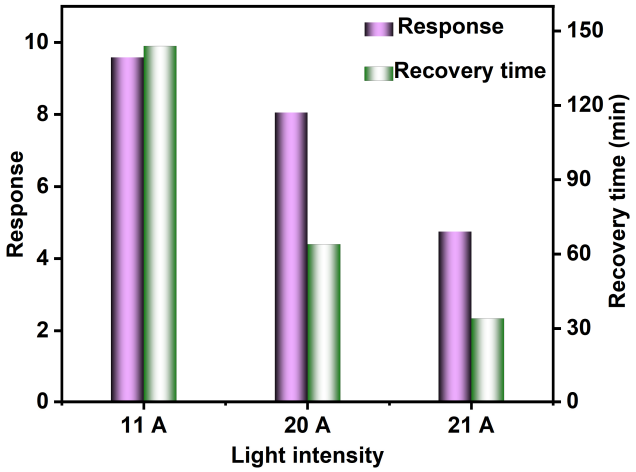

Figure S13. Comparison of response values and recovery times of the material under different light intensities of Cu-COF-366-OCH_3.

Table S1 Compared with reported chemiresistive NH_3 sensing of MOFs and COFs materials at room temperature.

Materials	Concentration (C)	Response (R)	Ref.
Cu-OHTBN	80 ppm	11.3 ± 0.8%	3
$Cu_3(HHTP)_2$	100 ppm	390%	4
Zn@COF-3	50 ppm	9490%	5
Zn(TDA)-MOF	50 ppm	13710%	6
SnCOF3	4 ppm	1980%	7
Zn@TpBpy COFs	50 ppm	1043%	8
COF-5 nanosheets	10 ppm	246%	9
TAPB-BPDA COF3	100 ppm	23%	10
Cu-HHTP-20C	100 ppm	230%	11
Cu-HHTP 3D thin film	10 ppm	60.5%	12
$Cu_3(HITP)_2$	10 ppm	~2.5%	13
$Cu_3(HHTP)_2$	100 ppm	129%	14
$Cu_3(HHTP)(THQ)$	100 ppm	~20%	15
$P_2MeOPy/COF1$	50 ppm (20 ℃, 73% RH)	-70%	16
COF/κPVA	10 ppm	61%	17
c-MIL-125_50% Zn	50 ppm	26800%	18
Co/Cu-HHTP	100 ppm	73.8%	19
$Cu_3(HHTP)_2$	80 ppm	0.7 ± 0.3%	20
Cu-HHTP-10C	100 ppm	~240%	21
Cu-BHT -2 min	20 ppm	7.5%	22
Cu-TCNQ thin film	50 ppm	0.06%	23
Cu-BTC@GO-25	100 ppm	4%	24
NiPc-Ni	80 ppm	43% - 45%	25
Bi(HHTP)	40 ppm	58.4 ± 2%	26
$Cu_3(HHTP)_2@SnS_2$	10 ppm	~15%	27
Zn-MOF/GO	100 ppm	13.2%	28
$H\text{-}MOF_6$/MXene	10 ppm	1337%	29
Ti_3C_2Tx–PVDF–ZIF-67	25 ppm (35% RH)	10.56%	30
rGO/ZIF-8 (RZF-50)	10 ppm	15.98 %	31
Cu-BTC/PPy-rGO	50 ppm	12.4 %	32
ZIF-8/CNT	100 ppm	~20%	33
ZIF8-ZnO/rGO	10 ppm	260%	34
This work	**100 ppm**	**825.9%**	**-**

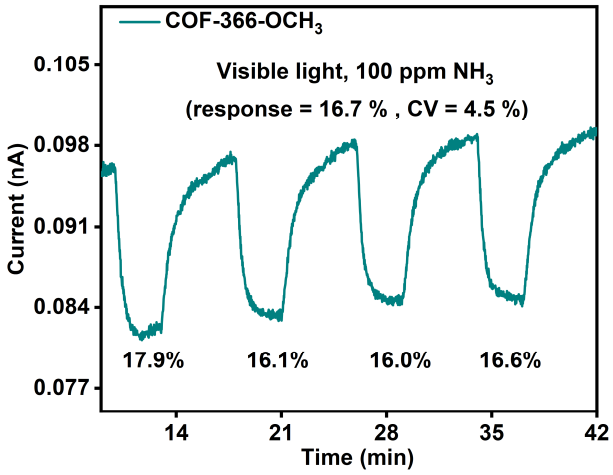

Figure S14. Response-recovery curve of COF-366-OCH_3 toward 100 ppm NH_3.

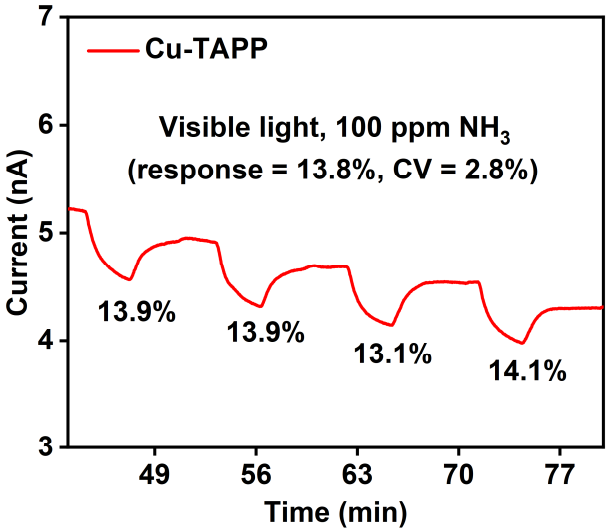

Figure S15. Response-recovery curve of Cu-TAPP toward 100 ppm NH_3.

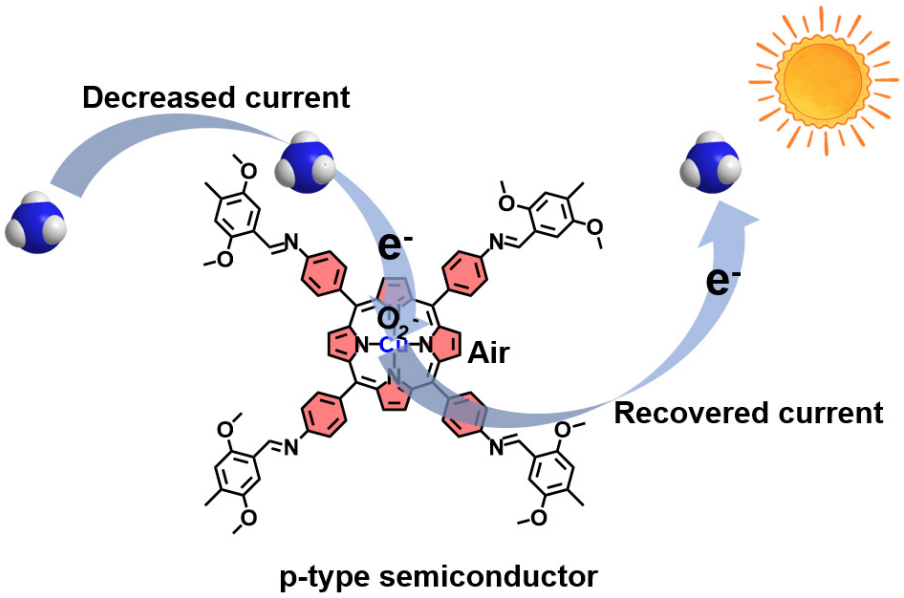

Figure S16. Possible sensing mechanism of Cu-COF-366-OCH_3.

Reference

1. Y.-L. Yang, Y.-R. Wang, G.-K. Gao, M. Liu, C. Miao, L.-Y. Li, W. Cheng, Z.-Y. Zhao, Y. Chen, Z. Xin, S.-L. Li, D.-S. Li and Y.-Q. Lan, *Chin. Chem. Lett.,* 2022, **33**, 1439-1444.
2. M. S. Yao, W. X. Tang, G. E. Wang, B. Nath and G. Xu, *Adv. Mater.,* 2016, **28**, 5229-5234.
3. Z. Wang, X. Ye, Y. Zhang, Q. Yang, K. Gao, Z. Li, H. Zhuo, Z. Wang, J. Liu, H. Yuan, K. Fan, Z. Meng and X. Shang, *J. Mater. Chem. A,* 2025, **13**, 27115-27124.
4. Y. Liu, F. Tian, J. A. Covington, Z. Wu, L. Hu and H. Li, *ACS Sens.,* 2025, **10**, 4045-4050.
5. S. B. Nallamalla, N. K. Katari, A. J. M. Reddy, S. B. Jonnalagadda and S. B. Manabolu Surya, *RSC Adv.,* 2025, **15**, 16708-16723.
6. P. Loomba, S. Nallamalla, K. Suresh, J. M. R. A, S. Rana, N. K. Katari and S. S. B. Manabolu, *J. the Indian Chem. Soc.,* 2025, **102**, 101756.
7. C. Liang, P. Li and S. Yu, *Ceram. Int.,* 2025, **51**, 21226-21234.
8. A. Mei, M. Zhou, W. Zhang, Y. Bao, Y. Liu and W. Chen, *Chem. Eng. J.,* 2025, **514**, 163087.
9. Z. Yang, A. Mei, W. Chen, Z. Wang, H. Guo and Y. Liu, *Sens. Actuators B: Chem.,* 2023, **392**, 134051.
10. F. Niu, Z.-W. Shao, J.-L. Zhu, L.-M. Tao and Y. Ding, *J. Mater. Chem. C,* 2021, **9**, 8562-8569.
11. M. S. Yao, J. W. Xiu, Q. Q. Huang, W. H. Li, W. W. Wu, A. Q. Wu, L. A. Cao, W. H. Deng, G. E. Wang and G. Xu, *Angew. Chem. Int. Ed.,* 2019, **58**, 14915-14919.
12. Y. Lin, W. H. Li, Y. Wen, G. E. Wang, X. L. Ye and G. Xu, *Angew. Chem. Int. Ed.,* 2021, **60**, 25758-25761.
13. M. G. Campbell, D. Sheberla, S. F. Liu, T. M. Swager and M. Dincă, *Angew. Chem. Int. Ed.,* 2015, **54**, 4349-4352.
14. M. S. Yao, X. J. Lv, Z. H. Fu, W. H. Li, W. H. Deng, G. D. Wu and G. Xu, *Angew. Chem. Int. Ed.,* 2017, **56**, 16510-16514.
15. M. S. Yao, J. J. Zheng, A. Q. Wu, G. Xu, S. S. Nagarkar, G. Zhang, M. Tsujimoto, S. Sakaki, S. Horike, K. Otake and S. Kitagawa, *Angew. Chem. Int. Ed.,* 2019, **59**, 172-176.
16. X. Zhang, D. Ma, Y.-Q. Zhao, H. Shi, L. Tao and F. Niu, *ACS Appl. Polym. Mater.,* 2025, **7**, 5556-5564.
17. X. Chen, M. Zeng, T. Wang, W. Ni, J. Yang, N. Hu, T. Zhang and Z. Yang, *Sensors,* 2024, **24**, 4324.
18. E. Namratha, M. S. Surendra Babu and A. Jagan Mohan Reddy, *Chem. Phys. Lett.,* 2025, **869**, 142059.
19. Y. Jiang, X. Hou, Y. Zhou, B. Wang, T. Wang, L. Zhao, J. Wei, P. Sun and G. Lu, *ACS Materials Lett.,* 2024, **7**, 76-84.
20. M. K. Smith, K. E. Jensen, P. A. Pivak and K. A. Mirica, *Chem. Mater.,* 2016, **28**, 5264-5268.
21. A.-Q. Wu, W.-Q. Wang, H.-B. Zhan, L.-A. Cao, X.-L. Ye, J.-J. Zheng, P. N. Kumar, K. Chiranjeevulu, W.-H. Deng, G.-E. Wang, M.-S. Yao and G. Xu, *Nano Res.,* 2020, **14**, 438-443.
22. X. Chen, Y. Lu, J. Dong, L. Ma, Z. Yi, Y. Wang, L. Wang, S. Wang, Y. Zhao, J. Huang and Y. Liu, *ACS Appl. Mater. Interfaces,* 2020, **12**, 57235-57244.
23. M. Shafiei, F. Hoshyargar, J. Lipton-Duffin, C. Piloto, N. Motta and A. P. O'Mullane, *J. Phys. Chem. C,* 2015, **119**, 22208-22216.
24. N. A. Travlou, K. Singh, E. Rodríguez-Castellón and T. J. Bandosz, *J. Mater. Chem. A,* 2015, **3**, 11417-11429.

25. Z. Meng, A. Aykanat and K. A. Mirica, *J. Am. Chem. Soc.,* 2018, **141**, 2046-2053.
26. A. Aykanat, C. G. Jones, E. Cline, R. M. Stolz, Z. Meng, H. M. Nelson and K. A. Mirica, *ACS Appl. Mater. Interfaces,* 2021, **13**, 60306-60318.
27. Y. Huang, X. Zhang, S. Liu, R. Wang, J. Guo, Y. Chen and X. Ma, *Chem. Eng. J.,* 2023, **458**, 141364.
28. Z. M. Ali, M. E. El Sayed, A. Samir and M. N. Murshed, *J. Electro. Mater.,* 2024, **54**, 262-272.
29. K. S. Ranjith, S. Sonwal, A. Mohammadi, G. Seeta Rama Raju, M.-H. Oh, Y. S. Huh and Y.-K. Han, *J. Mater. Chem. A,* 2024, **12**, 26132-26146.
30. N. K. Arkoti and K. Pal, *ACS Sens.,* 2024, **9**, 1465-1474.
31. S. Gupta, C. Ravikant and A. Kaur, *Relat. Mat.,* 2024, **148**, 111473.
32. Y. Yin, H. Zhang, P. Huang, C. Xiang, Y. Zou, F. Xu and L. Sun, *Mater. Res. Bull.,* 2018, **99**, 152-160.
33. W. Yan, S. Zhou, M. Ling, X. Peng and H. Zhou, *Inorganics,* 2022, **10**, 193.
34. D. Wang, M. Chi, D. Zhang and D. Wu, *J. Mater. Sci. Mater. Electron.,* 2020, **31**, 4463-4472.